

## Article

# Coupling Relationship between Rural Settlement Patterns and Landscape Fragmentation in Woodlands and Biological Reserves—A Case of Nanshan National Park

Bo Li <sup>1</sup>, Hao Ouyang <sup>1</sup>, Tong Wang <sup>2,\*</sup> and Tian Dong <sup>1</sup><sup>1</sup> School of Architecture and Art, Central South University, Changsha 410083, China<sup>2</sup> Management in the Built Environment Department, Architecture and Built Environment Faculty, Delft University of Technology, 2628 CD Delft, The Netherlands

\* Correspondence: t.wang-12@tudelft.nl

**Abstract:** Exploring the influence of settlement patterns on the landscape fragmentation in woodlands and biological reserves is key to achieving ecologically sustainable development. In this research, we chose the Nanshan National Park in Hunan Province, China, as a case study, to explore the influence mechanisms. First, we identified the biological reserves through the landscape security patterns of biological conservation. Second, we constructed a coupling coordination model to analyze the coupling relationship between the settlement patterns and landscape fragmentation in the woodlands and biological reserves. The analysis showed that, overall, the effect of the settlement area on the landscape fragmentation in the biological reserves was more pronounced, while the effect of the settlement spread and shape on the landscape fragmentation in the woodlands was more obvious. From a type-specific perspective, we analyzed the coupling relationship between the settlement patterns and (1) the landscape fragmentation in different woodlands and (2) the landscape fragmentation in the biological reserves, namely concerning *Leiothrix lutea* and *Emberiza aureola*. We found that the effect of the settlement patterns on the landscape fragmentation of the *Leiothrix lutea* biological reserve was more significant than that of the landscape fragmentation of its main habitat, the evergreen broad-leaved forest. The effect of settlement patterns on the landscape fragmentation of the *Emberiza aureola* biological reserve was more significant than that of the landscape fragmentation of its other habitats. In addition, the results demonstrated that the habitat protection of the woodlands was not a substitute for the systematic protection of biosecurity patterns. This research could assist in developing more efficient conservation measures for ecologically protected sites with rural settlements.

**Keywords:** settlement pattern; woodland ecosystem; landscape security pattern; landscape fragmentation; coupling coordination degree



**Citation:** Li, B.; Ouyang, H.; Wang, T.; Dong, T. Coupling Relationship between Rural Settlement Patterns and Landscape Fragmentation in Woodlands and Biological Reserves—A Case of Nanshan National Park. *Land* **2023**, *12*, 741. <https://doi.org/10.3390/land12040741>

Academic Editor: Jana Spulerova

Received: 21 February 2023

Revised: 20 March 2023

Accepted: 22 March 2023

Published: 25 March 2023



**Copyright:** © 2023 by the authors. Licensee MDPI, Basel, Switzerland. This article is an open access article distributed under the terms and conditions of the Creative Commons Attribution (CC BY) license (<https://creativecommons.org/licenses/by/4.0/>).

## 1. Introduction

Biodiversity is declining at an unprecedented rate in human history [1]. The average abundance of native species in most major terrestrial habitats has declined by at least 20% [2]. China is one of the most biodiverse countries in the world, but at the same time, it is also one of the most threatened countries in terms of biodiversity [3]. Chinese scholars have focused their research on biodiversity in three main areas. One has been to explore the mechanisms of biome maintenance and the relationship between biodiversity and ecosystem functionality [4,5]. The second has been to explore the practical methods of ecological reserve planning, investigation, and monitoring [6,7]. The third has been to explore the development of legal regulations for biodiversity conservation [8,9]. After recent decades of research and exploration, China has made significant achievements in biodiversity conservation, but biodiversity is still declining due to climate change and

human activities [3], so exploring the driving factors of biodiversity decline is an important aspect of biodiversity conservation in China.

Landscape fragmentation is one of the main causes of the sharp decline in biodiversity [1,10–12]. Landscape fragmentation is the process of dividing large and continuous landscape areas into smaller units and isolated patches [13,14]. It has many adverse effects on ecosystems, including increased ecosystem vulnerability, species mortality, and changes in species composition [15]. Landscape fragmentation is characterized by patch size, distance, shape, and boundary effects, and these factors can directly affect the composition, structure, and function of forest ecosystems [16–18]. For example, patches with a smaller proportion of the habitat within a buffer zone had lower connectivity, and patches with higher shape complexity and that were closer to the outside of the boundary had higher connectivity [19].

Many researchers suspect that although both natural and anthropogenic factors contribute to woodland landscape fragmentation, anthropogenic factors may contribute more significantly [20,21]. Frequent changes in land-use cover; the expansions of cash-crop cultivation [22]; the evolution of basic agricultural and construction lands [23]; increasing total population and irrigated area [24]; and policies to shrink ecological reserves [25] have led to the increased landscape fragmentation of woodlands. Cross-sectional studies of forest reserves in Romania [26], India [27], etc., have also confirmed this.

In addition, many studies have shown that the impact of settlement construction on landscape fragmentation in biological reserves has been more significant [28–30], and the interactions between settlement landscape patterns and natural ecosystems have been more complex [31], and the area, number, density, connectivity, shape similarity, and spatial organization patterns of settlements have had a significant impact on the size of biological communities and the species richness in biological reserves [32–35]. Ledda et al. used the Rural Building Fragmentation Index (RBF) and effective grid density and applied the mean-nearest-neighbor method to investigate the interactions between the spatial patterns of rural settlement construction and the landscape fragmentation [36]. Charlotte et al. used northern Wisconsin in the United States as an example and proposed that agricultural and grassland landscape fragmentation was associated with higher building densities and more dispersed building patterns in rural regions [37]. Li et al. used rural settlements in the Central Plains of China as a case study and suggested that rural settlements with small average patch sizes, poor homogeneity, and regular shapes could be conducive to reducing the fragmentation of biological reserves [38].

More specifically, woodland landscapes in mountainous areas have been characterized by high biodiversity and contain rich populations of plant and animal species [39], so the influence of woodland landscape fragmentation would be more complex, as compared to other types of landscapes [40]. Yet, there have been few studies on the association between rural settlements and woodland landscape fragmentation in mountainous areas. Moreover, most studies have analyzed woodland or habitat landscape fragmentation separately, overlooking the woodland landscape itself as the main habitat for many biological species [41,42] and the mutual influence between the two systems. However, whether there have been differences in the effects of rural settlement patterns on woodland landscapes versus habitat landscape fragmentation and the ways in which these specific differences manifest is not yet fully understood.

To repair fragmented landscape patches and protect internal ecosystem connections, a landscape-security-pattern approach has been widely adopted by most planners [43–46]. Landscape security patterns are certain spatial patterns that are composed of certain critical localities, locations, and spatial connections in the landscape. Landscape security patterns are important for maintaining and controlling certain ecological processes [47]. The landscape security patterns for biological conservation have achieved high spatially efficient biodiversity conservation goals, and they must be implemented for biological reserves with priority controls [48,49]. Existing studies on landscape security patterns have focused on two aspects: pattern identification [50–52] and ecosystem service–function analysis [53]. Among them,

studies related to landscape security patterns for biological conservation have focused on core biological habitat identification [54], biological migration-corridor construction [42], biological reserve management [55], and ecological risk assessment [56]. However, research on the influence of settlement patterns on landscape security patterns for biological conservation has not received sufficient attention.

National parks are established to conserve biodiversity and are large, nationally representative natural ecosystems [57]. China established the first 10 pilot areas of the national park system in 2016 and 5 national parks in 2021, which covered nearly 30% of the terrestrial nationally prioritized wildlife species, in order to protect the important biogeographic systems and ecological resources that have evolved naturally and are minimally affected by human activities [58]. Because of the lack of scientific and rational urban and rural construction and land-use policies, national parks and other biological reserves have experienced significant challenges, such as unclear boundaries, landscape fragmentation, and declining species abundance [59]. To achieve better ecosystem conservation, case studies have proposed improvement measures in terms of holistic conservation and the management of national parks, the optimization of ecological patch connectivity, ecological risk assessment, and vulnerability analysis [45,60,61]. However, few studies have analyzed biodiversity conservation in national parks from the perspective of settlement patterns. More specifically, the influence of rural settlement patterns on the landscape fragmentation in national parks needs to be further explored.

In summary, the impact of rural settlement patterns on woodlands and biological reserves in mountainous areas, especially in national parks, should be assessed by empirical studies. Therefore, this research chose Nanshan National Park in Hunan, China, as an empirical case study and analyzed the correlations between rural settlement patterns and landscape security patterns of the woodlands and biological reserves. This was achieved by identifying biologically conserved landscape security patterns, calculating the degree of the coupling coordination, and then comparing the similarities and differences between the woodlands and biological reserve landscape fragmentation under the influence of rural settlement patterns. By studying the relationship between rural settlement patterns and landscape fragmentation in China, we gained insight into the correlation between them and potential directions that could minimize the negative impact of rural construction on the environment and biodiversity for the protection rural ecological spaces. In addition, our findings could also facilitate the integration of rural landscape resources, realize the effective allocation of resources, and promote sustainable rural development.

## 2. Materials

### 2.1. Study Area

The study area was the Hunan Nanshan National Park, located in the southern part of Chengbu Miao Autonomous County, Hunan Province, between 25°58' and 26°42' N latitude and 109°58' and 110°37' E longitude, with a total area of about 632.94 km<sup>2</sup> (Figure 1). The topography of the study area slopes to the north from the east, west, and south, and is dominated by mountainous woodlands, accounting for 83.5% of the total area, with forest ecosystems represented by evergreen broad-leaved forests, inland wetland ecosystems, and southern alpine meadows. This region is also one of the main migratory routes for migrating birds in China and is an important conservation site and breeding ground for rare plants and animals. The region contains 6 townships and 43 administrative villages, with the number of rural settlements reaching 402 and a total population of 24,000. There are rich natural ecological resources in the region, but the landscape is highly fragmented, that is, there are more rural settlements and residents, and the ecological protection and the settlement construction and development has created significant conflicts.

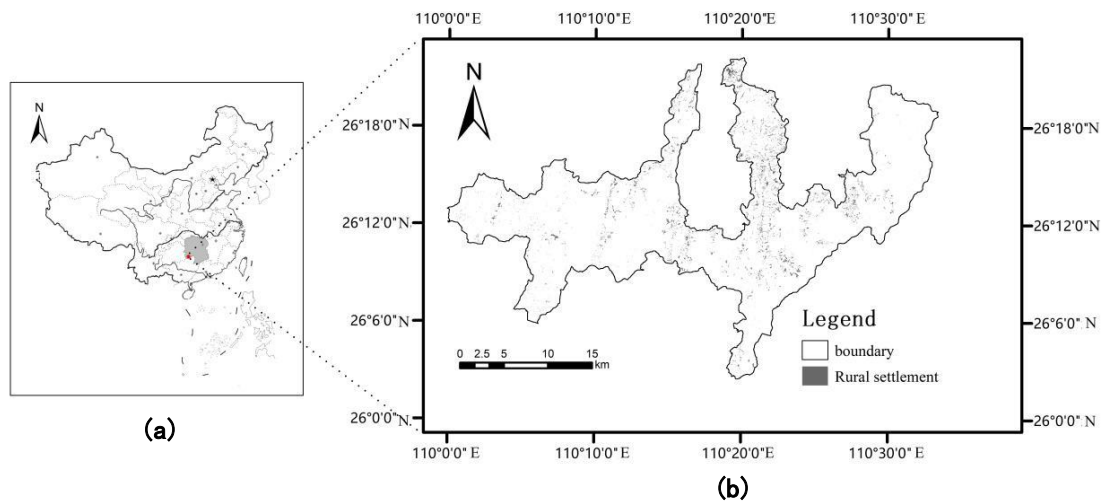


**Figure 1.** (a) Geographic location of the study area in China and (b) distribution of rural settlements in the study area.

## 2.2. Data Sources

Nanshan Park was identified as a national park pilot area in 2016, and to more clearly analyze the impact of settlement patterns on the landscape fragmentation of the biological reserve before the construction of the national park system, the Landsat 8 OLI\_TIRS remote sensing imagery and digital elevation model (DEM) database from 2016 was used in this study. They were obtained from the Geospatial Data Cloud website of the Computer Network Information Center of the Chinese Academy of Sciences (<http://www.gscloud.cn/>, accessed on 21 January 2019). After preliminary correction of remote sensing images and unsupervised classification interpretation, a raster map with a resolution of  $30\text{ m} \times 30\text{ m}$  was obtained for 7 land-use types: water system, village land, forest land, pastureland, agricultural land, dry land, and wetlands (Figure 2). The DEM elevation data were obtained by the natural intermittent-point-classification method. The spatial distribution data of forest resources were extracted from China Forestry Science Data Center (<http://www.cfsdc.org/web/zhuye/yhsysm.jsp>, accessed on 15 February 2019). The spatial distribution data of woodland-patch types, such as mixed forests, shrub forests, fir forests, and non-forest lands, in the study area were extracted (Figure 3).

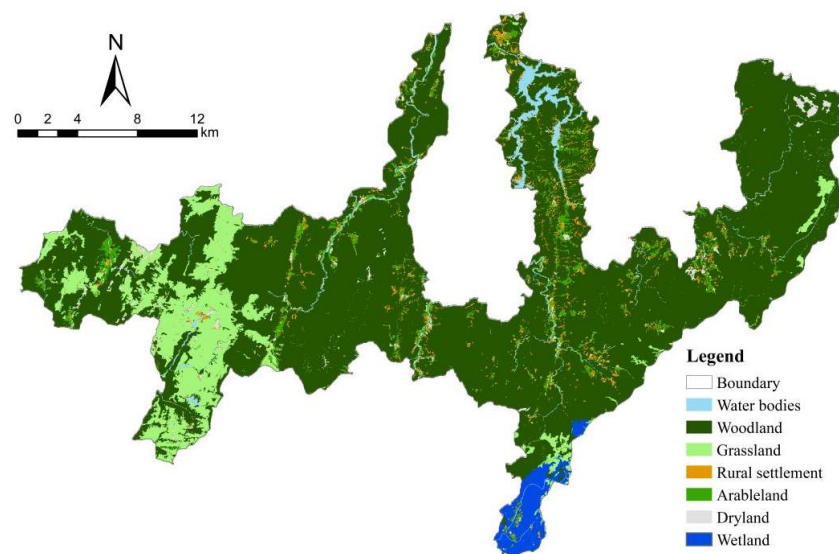


**Figure 2.** The 2016 land-use map of Hunan Nanshan National Park.

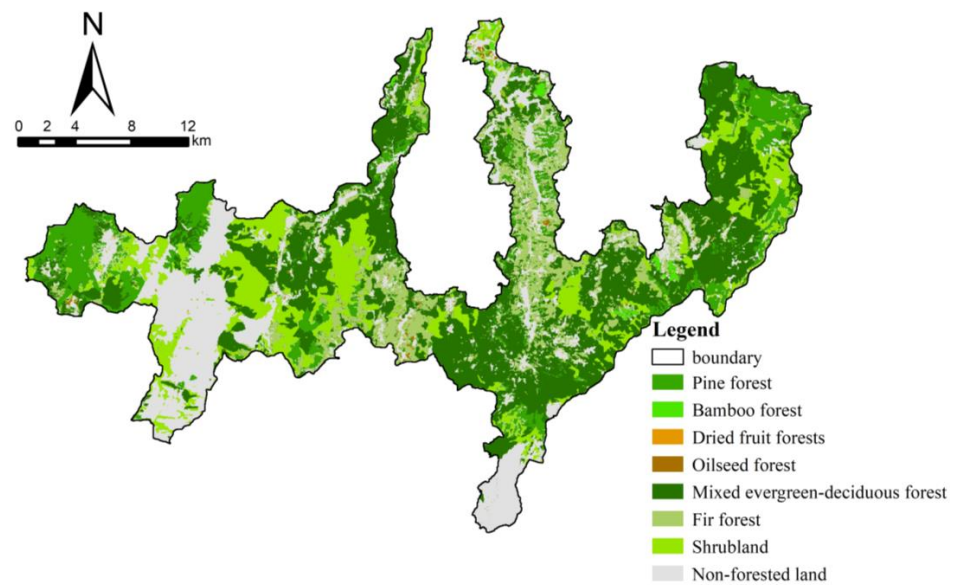


**Figure 3.** Distribution of forest resources in Hunan Nanshan National Park in 2016.

### 3. Methods

#### 3.1. Sample Area and Data Pre-Processing

##### 3.1.1. Sample Area Division

Grid analysis was applied for the landscape evaluation, environmental monitoring, and social analysis. The landscape units divided by the grid reflected the heterogeneity and spatial characteristics of the landscape, and at the same time, they were conducive to the integration and analysis of multi-sourced data. Therefore, concerning related studies [62–64], a 1 km \* 1 km grid system was constructed for the study area through the fishnet creation tool of ArcGIS10.6 (Figure 4).

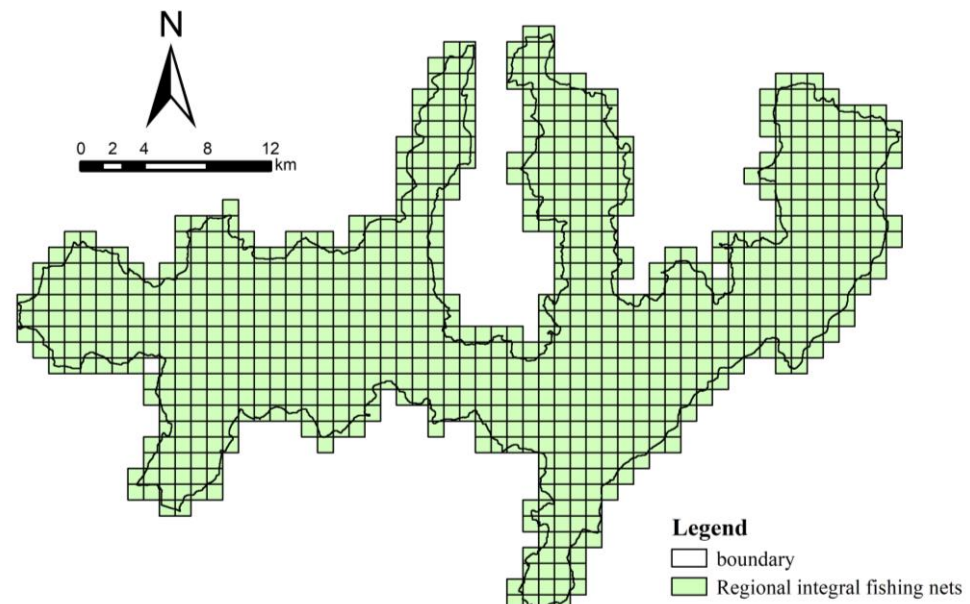


**Figure 4.** Regional overall fishnet construction.

##### 3.1.2. Indicator System Construction

To accurately measure and evaluate the coupling relationship between landscape fragmentation and settlement patterns in woodlands and biological reserves, this research relied upon a large amount of literature and the current situation of the study area, and we chose suitable landscape-pattern indexes that could characterize the spatial configuration and

structural composition of the landscape. Then, we constructed the landscape-fragmentation index system and settlement-pattern index system. Landscape pattern indicators were screened from two theoretical aspects. One was the landscape patch attributes, including patch area, perimeter, density, shape, type, etc. [51,65,66]. These attributes could characterize the interaction between regional landscape patches and the surrounding environment, which could then better reflect the condition of the regional ecological environment. The second was the relationship between landscape patches, including patch separation, aggregation, connectivity, etc. [65–68]. This type of index could reflect the material flow, spatial structure, and change trends in the landscape systems, and it was an important indicator for determining whether the regional landscape system could continue to exist and develop in a coordinated and stable manner. The calculation formula and ecological definition of the specific indexes are shown in Table 1.

**Table 1.** Landscape Fragmentation and Settlement Pattern Indicator System.

Indicator Type	Indicator Name	Ecological Meaning	Unit
Landscape-pattern index	Patch density (PD)	PD Indicates the number of patches per square kilometer of a landscape type [51,65].	%
	Landscape division index (DIVISION)	Division refers to the degree of separation of the individual distribution of different landscape patches in the same landscape type [66,67].	%
	Edge density (ED)	ED refers to the ratio between the total perimeter of all patch boundaries in the landscape and the total area of the landscape [51].	m/ha
	Aggregation index (AI)	AI is one of the indicators of the degree of fragmentation of plaques, with higher values indicating more significant aggregation and less fragmentation [51,65].	%
	Patch cohesion index (COHESION)	COHESION value is used to describe the connectivity between patch types, and the lower the proportion of a patch type, the closer the value is to zero [65,68].	–
	Largest patch area index (LPI)	LPI indicates the proportion of the largest patch in a given patch type that occupies the entire landscape area [51,68].	%
Rural Settlement-pattern index	landscape shape index (LSI)	LSI is one of the indicators of aggregation, and the more discrete the plaque type, the larger the LSI value [51]	–
	Contagion index (CONTAG)	CONTAG indicates the proportion of the landscape area occupied by each patch linkage type multiplied by the number of adjacent grid cells between these types as a proportion of the total number of adjacent grid cells [51,68]	%
	Mean patch size (Area_MN)	AREA_MN indicates the ratio of the total area of a patch type to the number of patches of that type, indicating the overall area size of the landscape patches [69,70].	ha

### 3.1.3. Data Standardization and Weights Determination

After passing through the grid mask, the raster data were imported into Fragstats 4.2 software, and the calculation was carried out in a square window of 100 m \* 100 m by the “moving windows” command, and the calculated raster layers were imported into ArcGIS software to calculate the average value of each landscape pattern indicator for all raster points within each grid, separately.

As different indicators were calculated, the results were prone to errors in quantitative units and orders of magnitude. To reduce the errors, the data needed to be standardized. In this research, the polar difference method was chosen for data standardization, and the processing method was as follows.

$$\text{Positive index : } X_{ij} = \frac{V_{ij} - \min_{1 \leq i \leq m} (V_{ij})}{\max_{1 \leq i \leq m} (V_{ij}) - \min_{1 \leq i \leq m} (V_{ij})} \quad (1)$$

$$\text{Negative index : } X_{ij} = \frac{\max_{1 \leq i \leq m} (V_{ij}) - V_{ij}}{\max_{1 \leq i \leq m} (V_{ij}) - \min_{1 \leq i \leq m} (V_{ij})} \quad (2)$$

where  $X_{ij}$  is the  $j$ th standardized value of the  $i$ th indicator,  $V_{ij}$  is the  $j$ th standardized value of the  $i$ th indicator, and  $m$  is the number of samples under study.

The entropy method uses information entropy to calculate the entropy value based on the degree of change in each indicator. The entropy value was used to correct the weights of each indicator and determine more objective weights [71–73]. Therefore, this study used the entropy method to calculate the weights of each indicator with the following formula.

$$P_{ij} = r_{ij} / \sum_{i=1}^m r_{ij} \quad (3)$$

$$e_j = -k \sum_{i=1}^m P_{ij} \ln P_{ij} \quad k = 1 / \ln m \quad (4)$$

$$w_j = (1 - e_j) / \sum_{j=1}^n (1 - e_j) \quad (5)$$

where  $r_{ij}$  is the value of the  $i$ th item of the  $j$ th index,  $p_{ij}$  denotes the index weight of the  $i$ th item of the  $j$ th index,  $e_j$  denotes the entropy of the  $j$ th index,  $w_j$  denotes the entropy weight of the  $j$ th index, and  $m$  is the number of sample areas.

### 3.2. Constructing Landscape Security Patterns for the Biological Reserves

To more comprehensively characterize the biological habitat of the study area, this paper selected the indicator species, *Leiothrix lutea* and *Emberiza aureola*, simulated their movement processes, constructed the landscape security patterns, and extracted the most ecologically valuable low-level security patterns in the biological reserve, which were used as the basic data for the subsequent analysis of the coupling and coordination between landscape fragmentation and settlement patterns. The principles used to select the indicator species included the following three considerations: first, representativeness, as the two types of indicator species were typical representatives of the biological taxa of migratory birds and resident birds, respectively; had a higher relative density in their biological taxa; were more sensitive to changes in the surrounding ecological environment; and have been significantly affected by environmental changes [74,75]; second, effectiveness, as the two types of species had an important ecological status and could represent the ecological value of their protected areas [76]; third, the contrast, as the distribution of the protected areas of the two bird species had little overlap, so they could more intuitively analyze the differences in the landscape pattern indicators on the influence of different species in the protected areas [77]. The specific construction steps were as follows.

#### 3.2.1. Selection of Ecological Source Sites

The native habitats of the *Leiothrix lutea* were extracted from the forest resource distribution map (mixed forest, shrub forest, and bamboo forest patches), and the main habitats of the *Emberiza aureola* were extracted from the land-use type and forest resource-distribution raster map (pasture, cultivated land, wetlands, and shrub forest patches).

### 3.2.2. Determination of Resistance Factors

Based on relevant studies of the resistance factors [78–82], we used the Delphi method, combined with a hierarchical analysis, to build the evaluation system of landscape-resistance value and weights for each index, as shown in Tables 2 and 3. By means of a questionnaire, 20 experts in the relevant fields were asked for their understanding of the evaluation factors. We standardized the above data through YAAHP hierarchical analysis software. To ensure the accuracy of the calculation results, a consistency test was performed, and the consistency index CI = 0.0000 was obtained, indicating that the decisions of the matrices were wholly consistent.

**Table 2.** The relative resistance-evaluation system.

Guideline Layer	The First Level Indicator Layer	Secondary Indicator Layer	Resistance Value	
			<i>Leiothrix lutea</i>	<i>Emberiza aureola</i>
Environmental Factors	Elevation	407–776 m	80	1
		776–1037 m	60	20
		1037–1288 m	40	40
		1288–1545 m	20	60
		1545–1985 m	10	80
	Land-use Type	Waters	80	40
		Woodland	1	1
		Pasture	40	20
		Village land	100	100
		Farmland	20	1
Interference factors	Distance from the settlement	Dryland, bare land	80	60
		Wetland	60	20
		0–500 m	100	100
		500–1000 m	80	80
	Distance from the water body	1000–1500 m	40	40
		>1500 m	1	1
		<500 m	80	-
		500–1000 m	60	-
	Distance from cultivated land	1000–1500 m	40	-
		>1500 m	20	-
<500 m		-	1	
500–1000 m		-	40	
		1000–1500 m	-	80
		>1500 m	-	100

**Table 3.** Resistance factor weights for indicative species.

Guideline Layer	The First Level Indicator Layer	Weighting Value			
		<i>Leiothrix lutea</i>		<i>Emberiza aureola</i>	
		Indicator Weights	Guideline Weights	Indicator Weights	Guideline Weights
Environmental Factors	Elevation	0.125	0.8333	0.125	0.75
	Land-use Type	0.875		0.875	
Interference factors	Distance from the settlement	0.6667	0.1667	0.1667	0.25
	Distance from the water body	0.3333		-	
	Distance from cultivated land	-		0.8333	

### 3.2.3. Resistance Surface Construction

This step was performed using the raster calculator tool in ArcGIS10.6 software. The spatial distribution of the integrated resistance surface was obtained by entering a formula consisting of the resistance value data of each indicator layer and its weight value, as well as the weight of the criterion layer.

### 3.2.4. Biological Reserve Security Pattern Construction

Using the cost distance tool in ArcGIS, the minimum cost distance of species expansion was obtained, and finally, the cumulative resistance value of each raster was classified into three categories: low, medium, and high, using the natural interruption-point-classification method. The category with the lowest cost resistance was selected as the core area of the biological reserve. Strategic nodes were identified to form a “strategic point-corridor-protected area” [83].

### 3.3. Calculation of the Landscape-Fragmentation Index

After deriving the weights of each index through the entropy weighting method, the landscape-fragmentation index of each sample area was calculated based on the standardized data with the following formula.

$$F_i = \sum_{j=1}^n w_j X_{ij} \quad (6)$$

where  $F_i$  is the landscape-fragmentation index of the  $i$ th sample area,  $w_j$  is the weight of the  $j$ th indicator, and  $X_{ij}$  is the  $j$ th standardized value of the  $i$ th indicator.

The spatial distribution data of forest resources and the overall protected area data, superimposed by two types of core protected areas of indicator species, were used as the basic data for the study of forest fragmentation and protected area fragmentation, respectively (shown in Figure 5). The grid with both landscape patches and settlement patches was selected as the sample area. Fragstats software was used to calculate each landscape-pattern index, and the weights of each landscape-pattern index were derived according to Equations (3)–(5) (Table 4). According to Equation (6), we calculated each landscape-fragmentation index of this area, and through ArcGIS software, we assigned the calculation results to the sample area, and through the natural interruption-point-classification method, we classified all the values into three categories: high, medium and low. As a result, we finally acquired the spatial distribution of the landscape-fragmentation index.

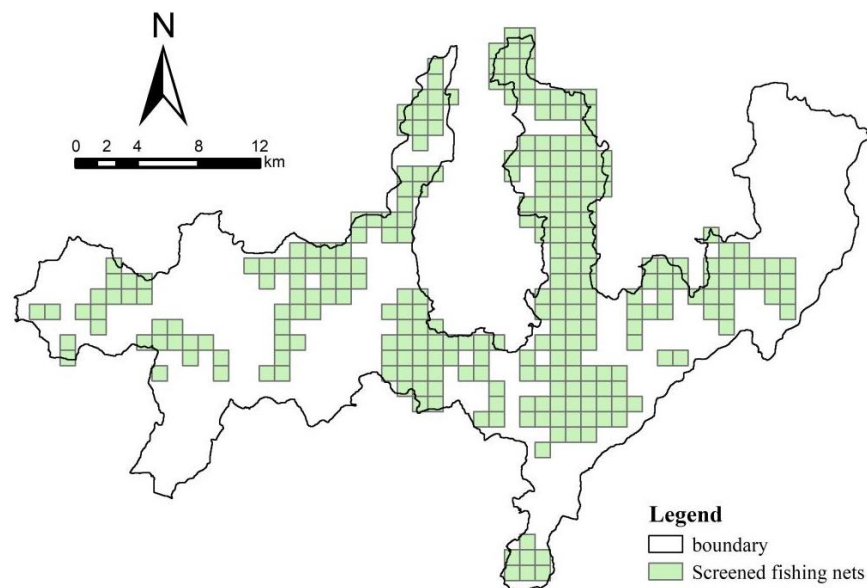


Figure 5. Sample patches.

**Table 4.** List of landscape-pattern-index weights.

Landscape Type		Landscape-Pattern Index Weights					
		AI	COHESION	DI	ED	LPI	PD
Woodland		0.2328	0.1514	0.1135	0.1710	0.1196	0.2118
Woodland type	Shrubland	0.1631	0.1634	0.1791	0.1586	0.1879	0.1479
	Fir Forest	0.1668	0.1524	0.1872	0.1592	0.2080	0.1263
	Evergreen broad-leaved forest	0.1861	0.1423	0.1755	0.1566	0.1991	0.1404
	Other forest lands	0.1636	0.1581	0.1780	0.1560	0.1974	0.1469
	Non-forested land	0.2057	0.1479	0.1565	0.1688	0.1670	0.1542
General Biological Reserve		0.2206	0.1332	0.1401	0.1749	0.1572	0.1740
Habitat type	<i>Leiothrix lutea</i> Biological Reserve	0.2412	0.1489	0.1448	0.1614	0.1456	0.1582
	<i>Emberiza aureola</i> Biological Reserve	0.1928	0.1605	0.1588	0.1651	0.1595	0.1633

### 3.4. Evaluation of the Coupling Coordination Degree

Coupling is a physical concept that indicates the degree of mutual influence and correlation between different systems through their interactions [84–86]. In this study, a coupling coordination model was used to explore the degree of interconnectedness between landscape fragmentation and settlement patterns, which was calculated as follows.

$$C_i = \sqrt{\frac{F_i \times G_i}{(F_i + G_i)^2}} \quad (7)$$

Since the degree of the landscape fragmentation and settlement patterns in different regions were differentiated and unbalanced, it would be easy to have a situation where one system was extremely high or extremely low, so relying on the degree of the coupling alone was prone to significant errors [87,88]. For this reason, the degree of the coupling could not represent the overall synergy between the two systems, and it was necessary to construct a coordination measurement model between landscape fragmentation and settlement-pattern indexes and then combine it with the degree of the coupling model to form a coupling coordination model, using the following formulas [89,90].

$$T_i = \alpha F_i \times \beta G_i \quad (8)$$

$$D_i = \sqrt{C_i \times T_i} \quad (9)$$

where  $C_i$  is the degree of the coupling of the landscape-fragmentation index and settlement-pattern index in the  $i$ th sample area;  $F_i$  is the index value of the landscape-pattern index in the  $i$ th sample area;  $G_i$  is the index value of the settlement-pattern index in the  $i$ th sample area;  $T_i$  is the integrated coefficient of coordination between landscape fragmentation and settlement pattern in the  $i$ th sample area;  $D_i$  denotes the coupling coordination between landscape fragmentation and settlement-pattern index in the  $i$ th sample area; and  $\alpha$  and  $\beta$  denote the weights of the landscape-fragmentation and settlement-pattern indexes, which were both taken as 0.5.

To distinguish the degree of the coupling between different types of the landscape fragmentation and settlement patterns, the coordination relationships between the systems were classified as five hierarchical types, according to the degree of the coupling coordination by using the uniform-distribution-function method, according to the relevant studies [85,86,91] (Table 5)

**Table 5.** Classification of coupled coordination assessment.

Degree of the Coupling Coordination Value (D) Range	Coordination States
0–0.2	Serious disorder
0.2–0.4	Mild coupling coordination
0.4–0.6	Primary coupling coordination
0.6–0.8	Favorable coupling coordination
0.8–1.0	Quality coupling coordination

The operational steps to determine the overall degree of coupling coordination between the fragmentation and settlement patterns were as follows: according to Equations (7)–(9), the degree of the coupling, the coordination index, and the degree of the coupling coordination were calculated for each sample area, and the percentage of the number of sample points in different value intervals was calculated according to the 5 types of the coupling coordination, as classified in Table 5.

The operational steps to determine the overall degree of coordination of different woodlands and biological reserves between the fragmentation and settlement patterns were as follows: by using the overlay tool of ArcGIS, the sample areas of each type of landscape and settlement patch were screened separately, and the coupling coordination between the fragmentation index and settlement-pattern index of each type of screened sample areas was calculated according to Equations (7)–(9), and the proportion of sample areas in different levels of each type was counted according to the criteria for each of the 5 types of the coupling coordination. The spatial distribution of each type of the coupling coordination was obtained by correlating the values of the coupling coordination to the corresponding sample areas.

## 4. Result

### 4.1. Biological Reserve Security Pattern

The landscape security patterns of *Leiothrix lutea* and *Emberiza aureola* were obtained by the ecological site selection, the resistance surface construction, and the minimum cumulative cost distance calculation, as illustrated in Section 3.2, and the results are shown in Figure 6.

The core area of the biosecurity pattern of the *Leiothrix lutea* was about 406.376 km<sup>2</sup>, accounting for 64.3% of the total study area, and was distributed in the eastern part of the study area and around the small rural settlements in the central western part of the study area, where there were a large number of woodland resources suitable for the habitat of the *Leiothrix lutea*. The buffer and coordination zones were distributed in the form of points near the rural settlements in the western and northern regions. The buffer and the coordination zones were primarily distributed in the form of points near the rural settlements in the west and the north, where the construction intensity was high and the woodland resources were small, which interfered more with the survival of *Leiothrix lutea*. The radiation paths were radially distributed from the low resistance convergence points inside the large landscape patches; the closer to the interior of the landscape patches, the more significant the density of the radiation paths. The ecological corridors connected the ecologically weak and rich areas along the edges of the landscape patches and the boundaries of the different types of the protected areas.

The core area of the *Emberiza aureola*'s biosecurity pattern was about 249.703 km<sup>2</sup>, accounting for 39.51% of the total study area, which was concentrated in the western shrublands and southern wetlands of the study area. The buffer and coordination zones were primarily distributed in the central, eastern, and northern regions, which comprised concentrated construction areas and tall forest areas that were not suitable for *Emberiza aureola*'s migration. The distribution of the radiation paths in the core area was denser, and the landscape patches were more strongly connected. The landscape ecological corridor crossed the core protected area to connect the ecological nodes.

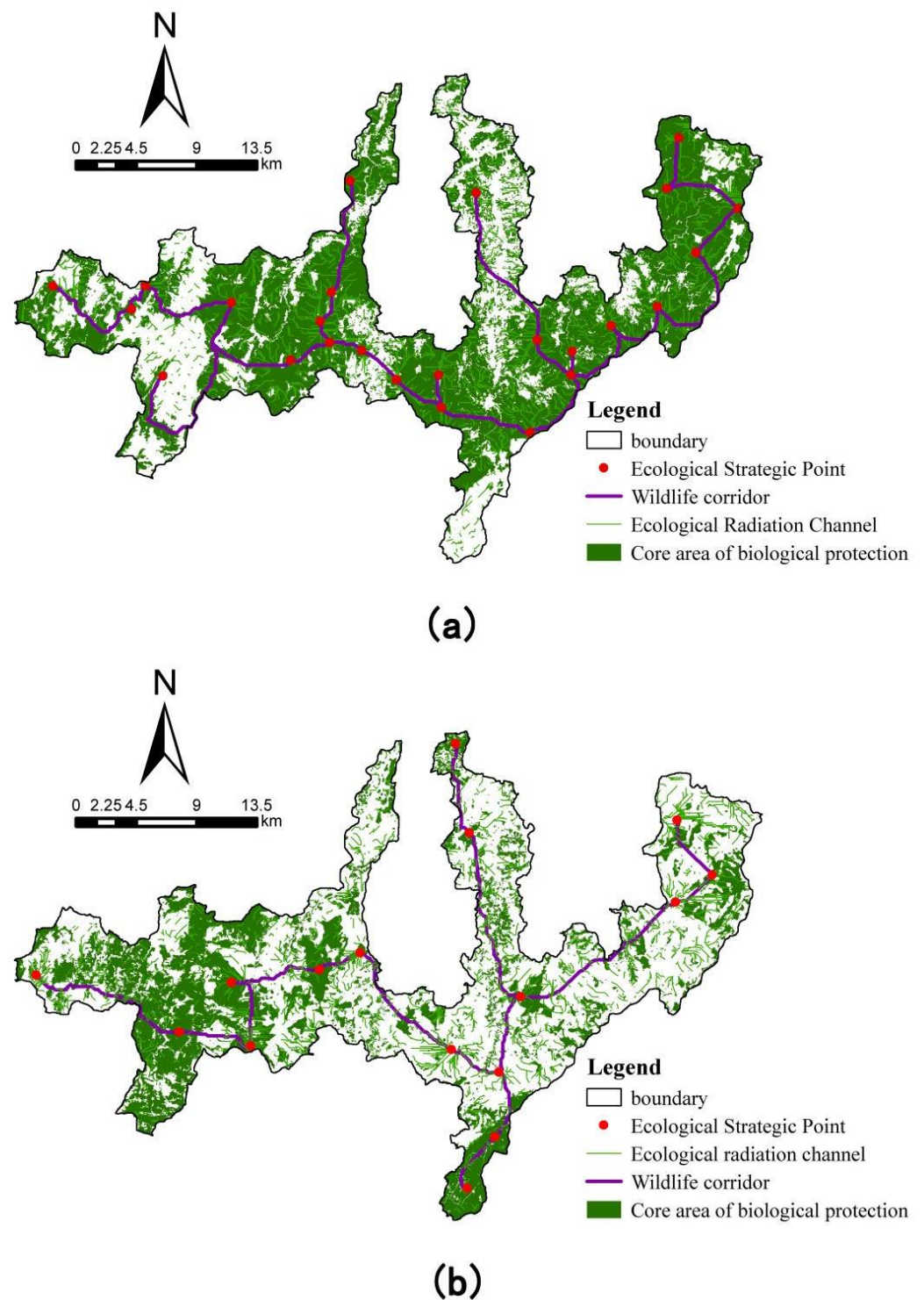


**Figure 6.** (a) *Leiothrix lutea* conservation security pattern map and (b) *Emberiza aureola* conservation security pattern map.

#### 4.2. Result of the Landscape-Fragmentation Index

By using ArcGIS software, the landscape-fragmentation index of the overall woodlands and biological reserves was obtained, as shown in Figure 7.

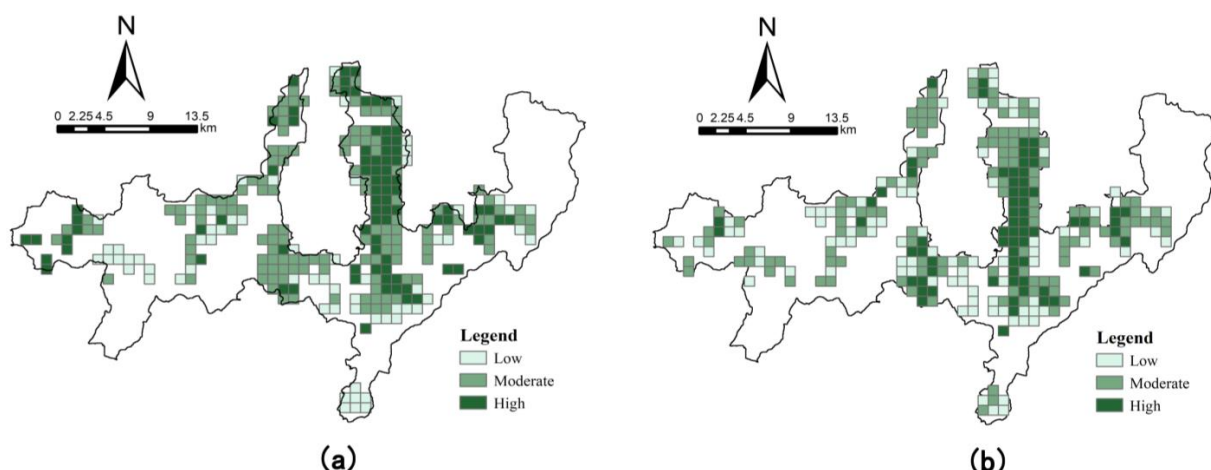


**Figure 7.** (a) Spatial map of woodland-landscape-fragmentation index and (b) distribution of overall biological reserve landscape-fragmentation index.

The samples in the high-value area that represented the two types of landscape fragmentation were similar in number, whereas the medium fragmentation of the woodlands was relatively high, and the area of low fragmentation accounted for a relatively small proportion, indicating that the overall fragmentation of the woodland landscape was more significant than that of the protected areas.

In terms of spatial distribution, both types of the landscape-fragmentation indexes were high in the east and low in the west, as well as low on all four sides, except for the central region. The landscape-fragmentation indexes of different types of biological reserves showed the characteristics of a multi-point distribution and were more scattered, while the landscape-fragmentation indexes of different types of woodlands had obvious homogeneous clustering. The high values were concentrated in the northeastern part of the study area, the middle values were concentrated in the middle and western regions, and the low values were primarily concentrated in the western and southern regions.

#### 4.3. Results of the Coupling Coordination Evaluation

##### 4.3.1. Overall Degree of the Coupling Coordination between the Fragmentation and Settlement Patterns

The percentages of sample points in different value intervals of the five types of the coupling coordination were calculated, and the results are shown in Table 6.

**Table 6.** The proportion of the number of D values of coupling coordination types.

Settlement-Pattern-Index Type	Evaluation Level of the Coupling Coordination	Woodland Fragmentation Index	Habitat Fragmentation Index
		Percentage of Different Levels of D-Value (%)	Percentage of Different Levels of D-Value (%)
AREA_MN	Serious disorder	1	0
	Mild coupling	1	1
	Primary coupling	11	11
	Favorable coupling	82	36
	Quality coupling	4	52
CONTAG	Serious disorder	1	1
	Mild coupling	9	9
	Primary coupling	29	27
	Favorable coupling	50	41
	Quality coupling	11	22
LSI	Serious disorder	2	5
	Mild coupling	19	35
	Primary coupling	46	38
	Favorable coupling	31	20
	Quality coupling	2	2

The calculated coupling coordination values were associated with the corresponding sample areas through the tabular-data-linking tool of ArcGIS, and the final spatial distributions of each type of the coupling coordination were obtained (Figure 8).

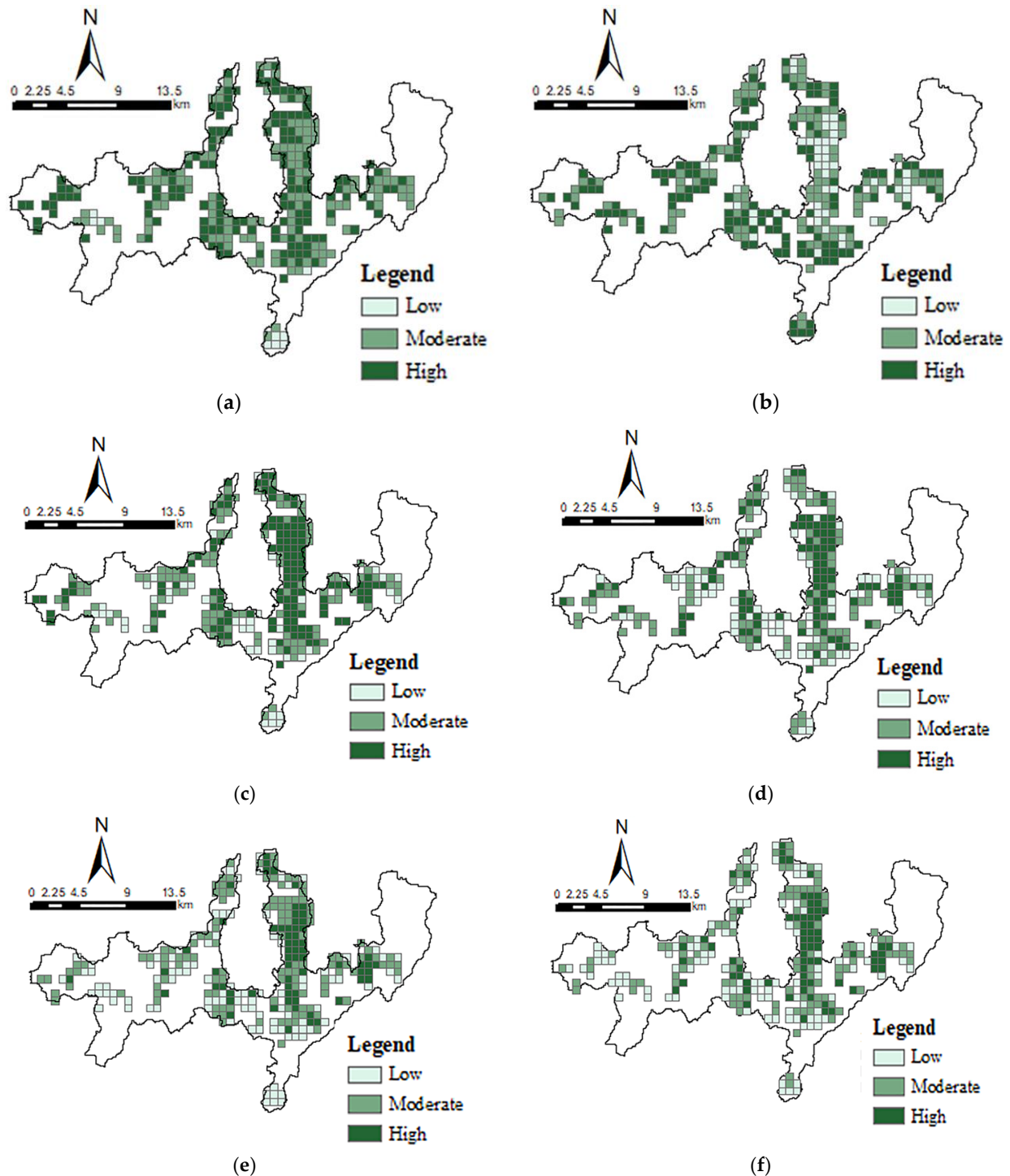


**Figure 8.** Spatial distribution of the coupling coordination between (a) woodland landscape-fragmentation index and AREA\_MN, (b) biological reserve landscape-fragmentation index and AREA\_MN, (c) woodland landscape-fragmentation index and CONTAG, (d) biological reserve landscape-fragmentation index and CONTAG, (e) woodland landscape-fragmentation index and LSI, and (f) biological reserve landscape-fragmentation index and LSI.

As shown in Table 6, more than 85% of the woodland and biological reserve patches had coupling coordination values between 0.6 and 1.0 with AREA\_MN and CONTAG, and less than 10% of the samples were in the low-value range, indicating that there was a strong degree of the coupling between the woodland fragmentation and the biological reserve patches and AREA\_MN and CONTAG in the study area. The results of the coupling coordination between the two types of fragmentation indexes and LSI showed that 60% of the sample areas were within the interval of primary and favorable coupling coordination, indicating that the external shape of the settlement development was influenced by the degrees of fragmentation in the woodland and biological reserve landscapes.

In terms of the spatial distribution, the high degrees of the coupling coordination between the two types of the landscape-fragmentation indexes and AREA\_MN were primarily distributed along the edges of the different types of land patches, while the high degrees of the coupling coordination with CONTAG and LSI were primarily distributed inside each patch group, showing a high trend in the east and a low trend in the west. There was an obvious concentration of high coupling coordination at Baiyun Lake Wetland Park in the north.

In terms of the characteristics of the distribution areas, the high values of the coupling coordination between the two types of the landscape-fragmentation indexes and AREA\_MN were distributed in areas with concentrated species habitats, such as the concentrated evergreen broad-leaved forests in the central west, the alpine pastures in the west, and the alpine wetlands in the south, while the high values of the coupling coordination with CONTAG and LSI were primarily distributed in areas with dense settlements and highly intense construction development in the northern region.

The main distribution intervals of the coupling coordination values between the settlement-pattern index and woodland/biological reserve fragmentation indexes were consistent. As compared to the forest land, the coupling coordination of the biological reserve fragmentation index with AREA\_MN and CONTAG was much higher in the quality coupling coordination interval, but the coupling coordination with LSI was lower in the primary and favorable coupling coordination interval. Based on the spatial distribution, the high coupling coordination values of the BPA fragmentation index with AREA\_MN were distributed in the central and western parts of the study area, while the high coupling coordination values of the forest land in this area showed a scattered multi-point distribution; the high coupling coordination values of the BPA fragmentation index with CONTAG and LSI were primarily distributed in the north.

#### 4.3.2. Evaluation of the Coupling Coordination between the Fragmentation Index and Settlement-Pattern Index for Each Type of Woodland and Biological Reserve

Because of the variability in the relationship between the degree of fragmentation of different landscape types and settlement patterns, this study further divided the woodlands into five categories: shrublands, fir forest, evergreen broad-leaved forest, other woodlands, and non-woodlands. Other woodlands were defined by a superimposed synthesis of smaller woodlands, such as pine forests and dry fruit forests, and non-woodlands were primarily the synthesis of land types other than woodlands, such as croplands and wetlands. The biological reserves were the core reserves of the indicator species *Leiothrix lutea* and *Emberiza aureola*, which were used to study the coupling and coordination relationships between the fragmentation of different landscape types and their settlement-pattern index.

According to the steps in Section 3.4, the proportions and spatial distributions of sample areas at different levels for different types of woodlands (shown in Table 7) and biological reserves were obtained (shown in Figure 9).

**Table 7.** Percentage of the number of different levels of D-values in the coupled coordination of specific types of woodlands and biological reserves.

Settlement-Pattern Index Type	Evaluation Level of the Coupling Coordination	Percentage of Forest Land Type D Value (%)					Percentage of D-Value of Biological Reserve Types (%)	
		Shrubland	Fir Forest	Evergreen Broad-Leaved Forest	Other Forest Lands	Non-Forested Land	<i>Leiothrix lutea</i> Reserve	<i>Emberiza aureola</i> Reserve
AREA_MN	Serious Disorder	3	0	1	2	1	1	1
	Mild	31	1	4	16	1	1	3
	Primary	24	12	19	50	22	10	20
	Favorable	33	36	63	29	74	82	71
	Quality	9	51	12	2	3	7	5
CONTAG	Serious Disorder	6	1	2	4	2	1	2
	Mild	35	9	8	26	11	7	13
	Primary	36	27	30	42	32	27	29
	Favorable	21	40	51	25	43	52	41
	Quality	1	23	9	3	12	13	16
LSI	Serious Disorder	7	5	3	10	3	1	5
	Mild	53	24	18	37	24	20	21
	Primary	30	38	44	39	44	42	43
	Favorable	9	29	35	13	26	34	28
	Quality	1	3	0	1	3	3	4

The results of the analysis of the settlement-pattern index showed that AREA\_MN had the highest coupling coordination with all landscape types of fragmentation, CONTAG the second, and LSI the lowest, which were consistent with the relationships between the coupling coordination of the fragmentation index and settlement-pattern index for the overall woodlands and biological reserves.

By comparing the coupling coordination models of the two types of biological reserves, the following conclusions were obtained. In terms of the percentages of the coupling coordination indexes, the degrees of coupling coordination between the landscape-fragmentation index and the settlement-pattern index were higher in the *Leiothrix lutea* reserve than in the *Emberiza aureola* reserve, and the differences between the two were the largest, in terms of the coupling coordination relationship, with AREA\_MN.

In terms of the spatial distribution, the coupling coordination between the fragmentation and AREA\_MN in the *Leiothrix lutea* reserve had a scattered distribution, while the coupling coordination between the landscape fragmentation and AREA\_MN in the *Emberiza aureola* reserve was high in the western and eastern regions. The spatial distribution of the coupling coordination between the fragmentation and CONTAG and LSI in the *Leiothrix lutea* reserve was more evenly distributed, showing a core of aggregated high values and gradually decreasing values along the periphery, while the coupling coordination of this aspect in the *Emberiza aureola* reserve was more spatially distributed in different regions, with a small clustering of high values in the north and more staggered values elsewhere.

By comparing the coupling coordination model of the landscape fragmentation of all woodland types, we found that the coupling coordination of the fir fragmentation index, with AREA\_MN and CONTAG, was the highest in terms of index values, and the sample areas with coupling coordination more significant than 0.6 accounted for more than 60%. From the spatial distribution, the coupling coordination of the fir forest, the evergreen broad-leaved forest, and other woodlands with AREA\_MN showed a high trend around the middle and low trend, while the coupling coordination with CONTAG and LSI were high around the middle, while the coupling coordination between the shrublands fragmentation and the three types of settlement-pattern indexes were high in the western and the eastern regions.

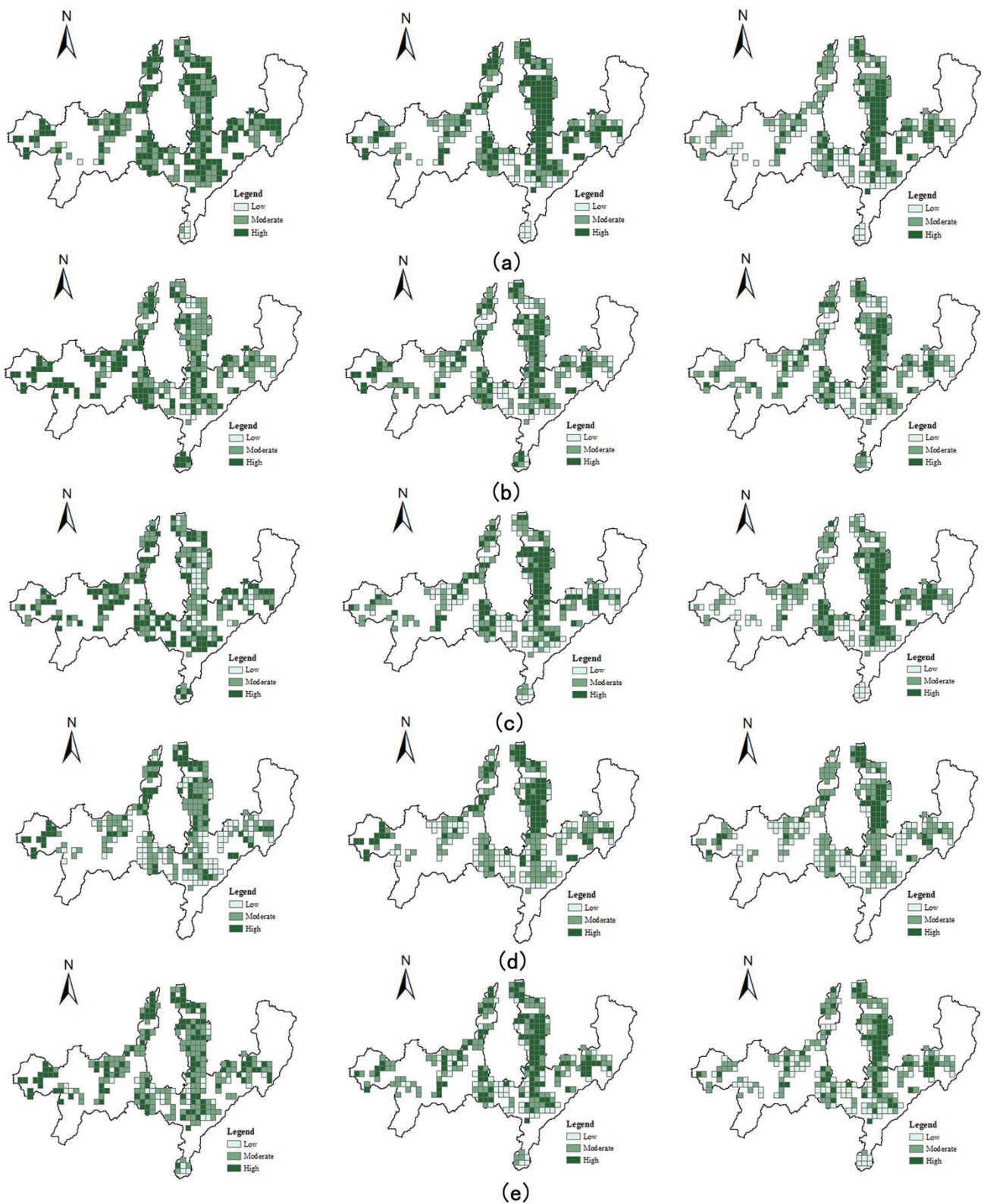
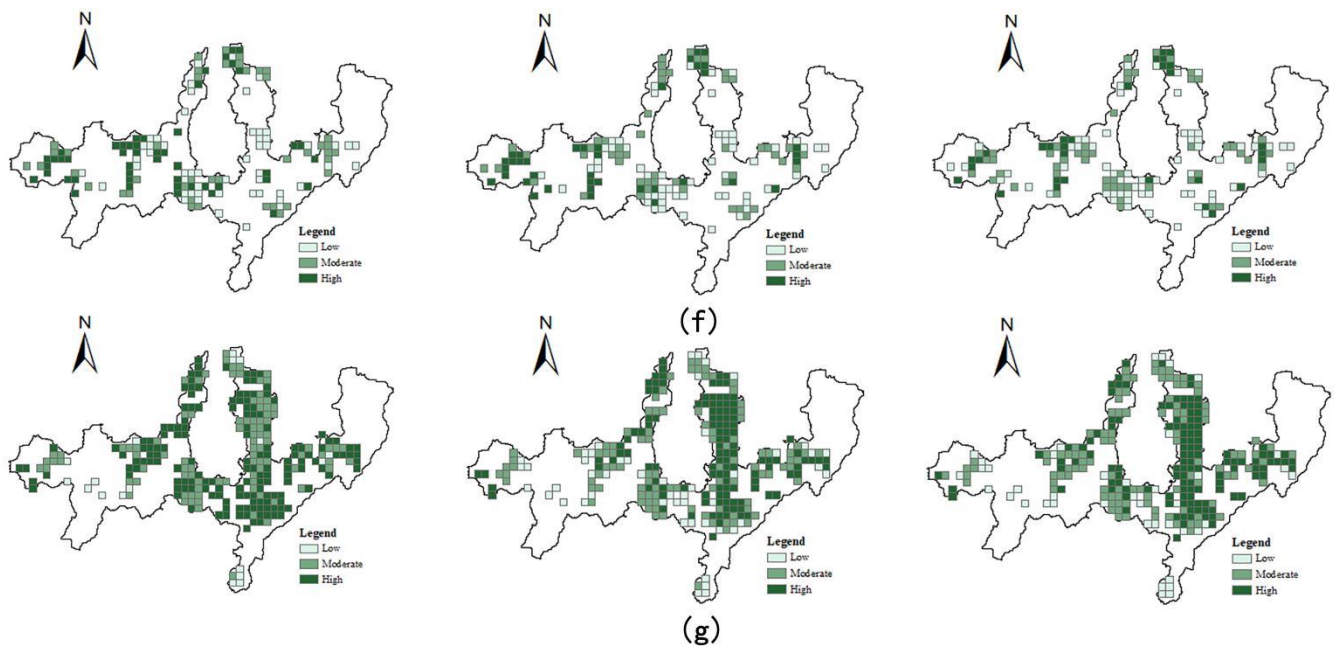


Figure 9. Cont.



**Figure 9.** Spatial distribution maps of the coupling coordination of (a) *Leiothrix lutea* bio-reserve, (b) *Emberiza aureola* bio-reserve, (c) fir forest, (d) other woodlands, (e) non-woodlands, (f) shrublands, and (g) mixed evergreen broad-leaved forest with the settlement-pattern indexes AREA\_MN, CONTAG, and LSI, respectively (left to right).

Combining the results of all woodland types, we found that AREA\_MN and CONTAG had higher coupling coordination with the landscape-fragmentation indexes of the fir forest, the evergreen broad-leaved forest, the non-woodlands, *Leiothrix lutea*, and *Emberiza aureola* reserve, indicating a stronger correlation between the average settlement patch areas and these systems. In terms of the numerical comparison, the overall coupling coordination between the fragmentation index and the settlement-pattern index was higher for the *Leiothrix lutea* reserves than for the evergreen broad-leaved forests, while the overall coupling coordination between the fragmentation index and the settlement-pattern index was slightly lower for the *Emberiza aureola* habitats than for the non-forested lands, but higher than for the shrublands.

## 5. Discussion

### 5.1. Settlement Patterns and Fragmentation of Woodlands and Biological Reserves

The present study confirmed that the settlement area, the shape index, and the spreading index had a more significant coupling relationship with the degree of the landscape fragmentation in woodlands and biological reserves, which was consistent with the findings of Zhu et al. [92] and Xu et al. [93]. However, the existing studies did not analyze the specific manifestations of the differences in the effects of settlement indicators on woodlands and biological reserves. In this study, by analyzing the model of the coupled and coordinated relationships between the landscape-fragmentation index and the settlement patterns in the woodlands and the biological reserves, we found that the influence of the settlement area on the landscape fragmentation was more significant along the edges of landscape patches and in the dense landscape patches. The degree of influence on the settlement aggregation and the development shape on the landscape fragmentation were more significant inside large landscape patches and in dense settlements. As stated in other studies, there was a stronger effect along the edges of the landscape patches [94,95], which increased the prominence of the landscape fragmentation caused by the encroachment of settlement construction on woodlands and biological reserves. At the same time, the outward expansion of settlements tended to create an inward squeeze on other landscape patches, causing more landscape patches to change from continuous to fragmented [96], producing more patchy edges

and changing the spatial properties of the landscape patches [97]. However, Zhang et al. argued that the expansion of settlement areas had a more significant effect on the landscape fragmentation in areas where construction activities were concentrated [98], probably because their study had not considered the differences in the influences on topography by construction activities. Furthermore, in mountainous areas, settlement construction is more obviously influenced by topography, and the compactness of settlement structures and the establishment of inter-settlement connections are more damaging to the integrity of the landscape patches directly. The development of transportation networks and complex settlement shapes in mountainous areas has led to a stronger disorderly fragmentation of the original landscape patches, seriously impacting the cycle of regional ecological functions [92]. While rural settlement roads can extend to higher heights, steeper slopes, and more sensitive habitats than urban roads [99], the length and spatial distribution of the rural roads largely complicate the landscape and ecological impacts [29], resulting in the landscape fragmentation of woodlands and biological reserves.

The comparison of the two types of models showed that the contribution of settlement sizes to the landscape fragmentation in the biological reserves was stronger, while settlement compactness and shape had a more pronounced impact on the landscape fragmentation of woodlands. This also reflected that the effects of settlement construction on indicator species habitats and biosecurity patterns had been different. Some settlement construction measures that were less associated with biotic habitat landscape fragmentation could have a more significant impact on biosecurity patterns. This was similar to the conclusions of Ledda et al. [36] and Charlotte et al. [37], but differed from the findings of Lockhart et al. [100]. The reason could be that the encroachment of settlements on biological reserves tended to disperse biological communities, that would then form numerous small groups [101,102], and the area differences between the small groups, the complexity of their migration trajectories, the increase in the stopover nodes, and the more dispersed community structure directly modified the overall biosecurity patterns, which in turn increased the landscape fragmentation of the biological reserves. The extension of the settlement shape and the changes in its compactness were more direct obstacles to the interaction between woodland patches, limiting each patch to passively extend in a direction with the least resistance and thereby producing many small woodland patches of different shapes and affecting the degree of the landscape fragmentation.

Therefore, when carrying out the construction of a mountain settlement, the overall construction area should be reasonably controlled, and the degree of aggregation of ecological landscape patches should be increased by measures, such as concentrating and merging rural greenways and parks, meadows, and forest patches, thereby reducing the dominance of construction land patches [92]. At the same time, the expansion of a mountain settlement area should be a considerable distance away from large centralized biological reserves, and the cluster development model should allow disturbance areas generated by adjacent settlements to overlap, thus minimizing the areas affected [103] and ensuring the remaining landscape would be more suitable for forest and wildlife, especially species that are sensitive to human disturbance [104].

### 5.2. Settlement Patterns and Fragmentation of Various Types of Woodlands and Two Types of Biological Reserves

By analyzing the coupling relationship between the landscape fragmentation and the settlement patterns in specific types of woodlands and biological reserves, we found that the relationship between the landscape fragmentation and the settlement patterns in biological reserves of indicator species differed significantly, regarding the type of woodlands they had primarily inhabited. Specifically, the landscape fragmentation of the *Leiothrix lutea* reserves was more significantly affected by the settlement patterns than the evergreen broad-leaved forests. The values with more significant correlations were distributed at the junction of the core, buffer, and coordination zones, and in areas with more radial paths in the landscape. As Ramellini et al. [102] and Herrando et al. [105] had demonstrate, *Leiothrix*

*lutea* populations showed exponential expansion: the closer they were to the population concentrations, the more prominent the impact of the settlement construction had on their survival and habitat. The fragmentation of the landscape of the *Emberiza aureola* reserve was less affected by the settlement patterns than the non-woodland landscapes and more affected than the shrubland landscapes, and the areas that were more strongly associated with the settlement areas were primarily distributed within the core biological conservation area. The areas that were more strongly associated with the settlement spread and shape were distributed in a band across the middle, which largely coincided with the main north–south longitudinal landscape corridor [80].

There were also significant differences in the effects of the fragmentation caused by the settlement patterns on the biological reserves of the different bird species. *Leiothrix luteas* are resident birds, and the landscape fragmentation along the edges of their protected areas was more significantly affected by the settlement patterns because the differences in the intensities of the settlement construction made the resistance values along the edges of their protected areas more variable and less connected. *Emberiza aureolas* are migratory birds, and the landscape fragmentation in the central part of their protected areas was more affected by the settlement patterns. Because they gather in flocks during migration [106,107] and choose continuous and safe migration paths in central areas of habitat patches with less human activity [108,109], changes in the shape and the compactness of the human settlements and the transportation facilities between settlements were more likely to affect the resistance at the various nodes along the migration path, resulting in the habitat macro-patches being more fragmented.

In terms of the spatial differentiation, the effect of the settlement area on the landscape fragmentation in the biological reserves was more prominent within the core of the reserve, while the effect of the settlement spread and shape on the landscape fragmentation in the biological reserves was more prominent within the coordination zone. The reason may have been due to biological core reserves being more likely to shape the characteristics of regular landscape environments, resulting in settlement spreading having a more significant impact on the overall area. However, the buffer zone of the biological reserve had to manage the material input from the core area and complete the material output with the coordination area, so it was more influenced by the shape of the settlement and the connection relationships. In addition, in areas rich in woodland types, the coupling relationship between each settlement index and landscape fragmentation was not significant. It was possible that the over-mixing of woodland types created too much scattering in the internal system, resulting in a more ambiguous interrelationship between the woodland fragmentation and the settlement patterns.

Therefore, the construction of settlements in mountainous forested areas should not only consider the integrity of the woodland landscape patches but also the landscape security patterns of indicator species. Along the edges of the *Leiothrix lutea* reserve and the core part of the *Emberiza aureola* reserve, the settlement area should be minimized and the construction intensity reduced.

## 6. Conclusions

This study applied the landscape ecological security pattern and a coupled coordination model to analyze and evaluate the correlations between the landscape fragmentation and the settlement patterns in mountainous woodlands and biological reserves in terms of both pattern indicators and spatial differentiation. It also explored the relationship between the fragmentation and the settlement patterns in different landscape types and indicator species, with the following findings.

(1) The biosecurity patterns of two indicator species in the study area were constructed by using the MCR model, in which the core protected areas of *Leiothrix lutea* were distributed in the eastern part and around the rural settlements in the central west. The radial paths were distributed from the low-resistance convergence points inside the large landscape patches outwards, and the ecological corridors were shown to connect the ecologically

weak and rich areas along the edges of the landscape patches and the boundaries of the core areas. The radiation paths in the core area were more densely distributed, and the landscape patches were more strongly connected. The ecological corridor crossed the core protected area and connects all ecological nodes.

(2) By constructing a coupled coordination model between the woodlands, the biological reserves, and the settlement patterns, we found that the degree of the landscape fragmentation was more correlated with the average patch size of the settlement at the edge of the junction of each land type or in the area where the landscape patches were concentrated, while the degree of the landscape fragmentation was affected by the connectivity, the dispersion, and the development shape of the settlements within each group or within the area where the rural construction and development were concentrated. There were obvious clustering cores with a high coupling coordination in areas where both the natural landscape fragmentation and the artificial construction intensity were high. By comparing the results of the two models, we found that the landscape fragmentation in the biological reserves was more strongly correlated with the average patch area of the clusters and the degree of cluster connectivity and agglomeration, while the correlation between patch fragmentation in the woodlands and the shape of the clusters was more obvious.

(3) By constructing a model of the coupling coordination among each type of woodlands, biological reserves, and settlement patterns, we concluded that the coupling coordination between the fir forest and the settlement pattern was the highest. The degree of fragmentation was more correlated with the area; the degree of aggregation and dispersion; and the development shape of the settlement in the *Leiothrix lutea* reserve than in the *Emberiza aureola* reserve. The landscape fragmentation was more significantly influenced by the settlement patterns in the *Leiothrix lutea* reserve than in the broad-leaved evergreen forest, which was its main habitat. The landscape fragmentation was less influenced by the settlement patterns in the *Emberiza aureola* reserve than in the non-woodland areas, and more influenced by shrublands, which was its main habitat.

The study of the settlement patterns on the landscape fragmentation in woodland and biological reserves demonstrated the differences in the conservation values for biodiversity conservation. For species whose primary habitat is woodlands, protecting woodland landscape diversity was not necessarily effective in protecting their habitat environment, and the changes in different settlement attributes could have different effects on the landscape. However, this research only studied the landscape patterns from a single period, which could not reveal the dynamic impact of settlement pattern development on landscape fragmentation. Our next study will combine multi-temporal data to carry out an in-depth analysis, provide suggestions for restoring fragmented landscape habitats and efficiently protecting biodiversity in mountainous woodlands, and propose optimization strategies for settlement planning, construction, and management.

**Author Contributions:** Conceptualization, B.L. and H.O.; methodology, T.W.; software, H.O.; validation, T.D., B.L. and H.O.; formal analysis, T.W.; investigation, B.L.; resources, H.O.; data curation, T.D.; writing—original draft preparation, H.O., B.L.; writing—review and editing, T.W., B.L.; visualization, B.L.; supervision, T.W., B.L.; project administration, T.D.; funding acquisition, T.W., B.L. All authors have read and agreed to the published version of the manuscript.

**Funding:** The APC costs are covered by Delft University of Technology.

**Data Availability Statement:** Not applicable.

**Conflicts of Interest:** The authors declare no conflict of interest.

## References

1. Di Giulio, M.; Holderegger, R.; Tobias, S. Effects of habitat and landscape fragmentation on humans and biodiversity in densely populated landscapes. *J. Environ. Manag.* **2009**, *90*, 2959–2968. [[CrossRef](#)]
2. Schmeller, D.S.; Niemelä, J.; Bridgewater, P. The Intergovernmental Science-Policy Platform on Biodiversity and Ecosystem Services (IPBES): Getting involved. *Biodivers. Conserv.* **2017**, *26*, 2271–2275. [[CrossRef](#)]

3. Wang, W.; Wang, W.; Feng, C.; Liu, F.; Li, J. Biodiversity conservation in China: A review of recent studies and practices. *Environ. Sci. Ecotechnol.* **2020**, *2*, 100025. [[CrossRef](#)]
4. Feng, G.; Mi, X.; Yan, H.; Li, F.Y.; Svenning, J.C.; Ma, K. CForBio: A network monitoring Chinese forest biodiversity. *Sci. Bull.* **2016**, *61*, 1163–1170. [[CrossRef](#)]
5. Xu, H.; Cao, M.; Wu, J.; Cai, L.; Ding, H.; Jun, L.; Yi, W.; Peng, C.; Lian, C.; Zhi, L.; et al. Determinants of Mammal and Bird Species Richness in China Based on Habitat Groups. *PLoS ONE* **2015**, *10*, e0143996. [[CrossRef](#)]
6. Mi, X.; Guo, J.; Hao, Z.; Xie, Z.; Guo, K.; Ma, K. Chinese forest biodiversity monitoring: Scientific foundations and strategic planning. *Biodivers. Sci.* **2016**, *24*, 1203–1219. [[CrossRef](#)]
7. Wu, J.; Xue, D.; Zhao, F.; Wang, Y. Progress of the Study on Investigation and Conservation of Biodiversity in China. *J. Ecol. Rural. Environ.* **2013**, *29*, 146–151.
8. Chen, C.; Park, T.; Wang, X.; Piao, S.; Xu, B.; Chaturvedi, R.K.; Fuchs, R.; Brovkin, V.; Ciaia, P.; Fensholt, R.; et al. China and India lead in greening of the world through land-use management. *Nat. Sustain.* **2019**, *2*, 122–129. [[CrossRef](#)] [[PubMed](#)]
9. Yang, R.; Yang, R.; Peng, Q.; Cao, Y.; Zhong, L.; Hou, S.; Zhao, Z.; Huang, C. Transformative changes and paths toward biodiversity conservation in China. *Biodivers. Sci.* **2019**, *27*, 1032–1040.
10. Diaz, S.; Settele, J.; Brondizio, E.S.; Ngo, H.T.; Agard, J.; Arneth, A.; Balvanera, P.; Brauman, K.A.; Butchart, S.H.M.; Chan, K.M.A.; et al. Pervasive human-driven decline of life on Earth points to the need for transformative change. *Science* **2019**, *366*, eaax3100. [[CrossRef](#)] [[PubMed](#)]
11. Kaboodvandpour, S.; Almasieh, K.; Zamani, N. Habitat suitability and connectivity implications for the conservation of the Persian leopard along the Iran-Iraq border. *Ecol. Evol.* **2021**, *11*, 13464–13474. [[CrossRef](#)]
12. Mohammadi, A.; Almasieh, K.; Nayeri, D.; Adibi, M.A.; Wan, H.Y. Comparison of habitat suitability and connectivity modelling for three carnivores of conservation concern in an Iranian montane landscape. *Landsc. Ecol.* **2022**, *37*, 411–430. [[CrossRef](#)]
13. Sahana, M.; Sajjad, H.; Ahmed, R. Assessing spatio-temporal health of forest cover using forest canopy density model and forest fragmentation approach in Sundarban reserve forest, India. *Model. Earth Syst. Environ.* **2015**, *1*, 49. [[CrossRef](#)]
14. Saunders, D.A.; Hobbs, R.J.; Margules, C.R. Biological Consequences of Ecosystem Fragmentation: A Review. *Conserv. Biol.* **1991**, *5*, 18–32. [[CrossRef](#)]
15. Ramanathan, V.; Chung, C.; Kim, D.; Bettge, T.; Buja, L.; Kiehl, J.T.; Washington, W.M.; Fu, Q.; Sikka, D.R.; Wild, M. Atmospheric brown clouds: Impacts on South Asian climate and hydrological cycle. *Proc. Natl. Acad. Sci. USA* **2005**, *102*, 5326–5333. [[CrossRef](#)]
16. Lima, B.C.; Francisco, C.N.; Bohrer, C.B.D. Landslides and forest fragmentation in the mountain range region of rio de janeiro state. *Cienc. Florest.* **2017**, *27*, 1283–1295. [[CrossRef](#)]
17. Magnago, L.F.S.; Rocha, M.F.; Meyer, L.; Martins, S.V.; Meira-Neto, J.A.A. Microclimatic conditions at forest edges have significant impacts on vegetation structure in large Atlantic forest fragments. *Biodivers. Conserv.* **2015**, *24*, 2305–2318. [[CrossRef](#)]
18. Tabarelli, M.; Da Silva, J.M.C.; Gascon, C. Forest fragmentation, synergisms and the impoverishment of neotropical forests. *Biodivers. Conserv.* **2004**, *13*, 1419–1425. [[CrossRef](#)]
19. Zhang, J.; Wang, X.; Xie, Y. Implication of Buffer Zones Delineation Considering the Landscape Connectivity and Influencing Patch Structural Factors in Nature Reserves. *Sustainability* **2021**, *13*, 10833. [[CrossRef](#)]
20. Jiang, W.G.; Lv, J.X.; Wang, C.C.; Chen, Z.; Liu, Y.H. Marsh wetland degradation risk assessment and change analysis: A case study in the Zoige Plateau, China. *Ecol. Indic.* **2017**, *82*, 316–326. [[CrossRef](#)]
21. Liu, C.J.; Zhang, F.; Johnson, V.C.; Duan, P.; Kung, H.T. Spatio-temporal variation of oasis landscape pattern in arid area: Human or natural driving? *Ecol. Indic.* **2021**, *125*, 107495. [[CrossRef](#)]
22. de Oliveira, B.R.; Carvalho-Ribeiro, S.M.; Maia-Barbosa, P.M. Maia-Barbosa, Rio Doce State Park buffer zone: Forest fragmentation and land use dynamics. *Environ. Dev. Sustain.* **2020**, *23*, 8365–8376. [[CrossRef](#)]
23. Penghui, J.; Dengshuai, C.; Manchun, L. Farmland landscape fragmentation evolution and its driving mechanism from rural to urban: A case study of Changzhou City. *J. Rural. Stud.* **2021**, *82*, 1–18. [[CrossRef](#)]
24. Xue, J.; Gui, D.W.; Zeng, F.J.; Yu, X.B.; Sun, H.W.; Zhang, J.; Liu, Y.; Xue, D.P. Assessing landscape fragmentation in a desert-oasis region of Northwest China: Patterns, driving forces, and policy implications for future land consolidation. *Environ. Monit. Assess.* **2022**, *194*, 394. [[CrossRef](#)] [[PubMed](#)]
25. Conceicao, E.O.; Garcia, J.M.; Alves, G.H.Z.; Delanira-Santos, D.; Corbetta, D.D.; Betiol, T.C.C.; Pacifico, R.; Romagnolo, M.B.; Batista-Silva, V.F.; Bailly, D.; et al. The impact of downsizing protected areas: How a misguided policy may enhance landscape fragmentation and biodiversity loss. *Land Use Policy* **2022**, *112*, 105835. [[CrossRef](#)]
26. Vorovencii, I. Quantifying landscape pattern and assessing the land cover changes in Piatra Craiului National Park and Bucegi National Park, Romania, using satellite imagery and landscape metrics. *Environ. Monit. Assess.* **2015**, *187*, 692. [[CrossRef](#)]
27. Reddy, C.S.; Sreelekshmi, S.; Jha, C.S.; Dadhwal, V.K. National assessment of forest fragmentation in India: Landscape indices as measures of the effects of fragmentation and forest cover change. *Ecol. Eng.* **2013**, *60*, 453–464. [[CrossRef](#)]
28. Compas, E. Measuring exurban change in the American West: A case study in Gallatin County, Montana, 1973–2004. *Landsc. Urban. Plan.* **2007**, *82*, 56–65. [[CrossRef](#)]
29. Liang, J.; Liu, Y.; Ying, L.X.; Li, P.; Xu, Y.; Shen, Z.H. Road impacts on spatial patterns of land use and landscape fragmentation in three parallel rivers region, Yunnan Province, China. *Chin. Geogr. Sci.* **2014**, *24*, 15–27. [[CrossRef](#)]
30. Ma, B.R.; Tian, G.J.; Kong, L.Q.; Liu, X.J. How China's linked urban–rural construction land policy impacts rural landscape patterns: A simulation study in Tianjin, China. *Landsc. Ecol.* **2018**, *33*, 1417–1434. [[CrossRef](#)]

31. de Castro-Pardo, M.; Azevedo, J.C.; Fernández, P. Ecosystem Services, Sustainable Rural Development and Protected Areas. *Land* **2021**, *10*, 1008. [[CrossRef](#)]
32. Heider, K.; Lopez, J.M.R.; Aviles, J.M.G.; Balbo, A.L. Land fragmentation index for drip-irrigated field systems in the Mediterranean: A case study from Ricote (Murcia, SE Spain). *Agric. Syst.* **2018**, *166*, 48–56. [[CrossRef](#)]
33. Lu, H.; Xie, H.L.; He, Y.F.; Wu, Z.L.; Zhang, X.M. Assessing the impacts of land fragmentation and plot size on yields and costs: A translog production model and cost function approach. *Agric. Syst.* **2018**, *161*, 81–88. [[CrossRef](#)]
34. Onilude, O.O.; Vaz, E. Data Analysis of Land Use Change and Urban and Rural Impacts in Lagos State, Nigeria. *Data* **2020**, *5*, 72. [[CrossRef](#)]
35. Wang, Y.H.; Li, X.B.; Lu, D.; Yan, J.Z. Evaluating the impact of land fragmentation on the cost of agricultural operation in the southwest mountainous areas of China. *Land Use Policy* **2020**, *99*, 105099. [[CrossRef](#)]
36. Ledda, A.; Serra, V.; De Montis, A. The Effect of Rural Buildings on Landscape Fragmentation in Natura 2000 Sites: A Case Study in Sardinia. *Sustainability* **2019**, *11*, 4695. [[CrossRef](#)]
37. Gonzalez-Abraham, C.E.; Radeloff, V.C.; Hammer, R.B.; Hawbaker, T.J.; Stewart, S.I.; Clayton, M.K. Building patterns and landscape fragmentation in northern Wisconsin, USA. *Landsc. Ecol.* **2006**, *22*, 217–230. [[CrossRef](#)]
38. Li, G.Y.; Jiang, C.H.; Du, J.; Jia, Y.P.; Bai, J. Spatial differentiation characteristics of internal ecological land structure in rural settlements and its response to natural and socio-economic conditions in the Central Plains, China. *Sci. Total. Environ.* **2020**, *709*, 135932. [[CrossRef](#)]
39. Bailey, S.A.; Haines-Young, R.H.; Watkins, C. Species presence in fragmented landscapes: Modelling of species requirements at the national level. *Biol. Conserv.* **2002**, *108*, 307–316. [[CrossRef](#)]
40. Pavlacky, D.C.; Anderson, S.H. Does avian species richness in natural patch mosaics follow the forest fragmentation paradigm? *Anim. Conserv.* **2007**, *10*, 57–68. [[CrossRef](#)]
41. Debusse, V.J.; King, J.; House, A.P.N. Effect of fragmentation, habitat loss and within-patch habitat characteristics on ant assemblages in semi-arid woodlands of eastern Australia. *Landsc. Ecol.* **2007**, *22*, 731–745. [[CrossRef](#)]
42. Cooper, C.B.; Walters, J.R. Independent effects of woodland loss and fragmentation on Brown Treecreeper distribution. *Biol. Conserv.* **2002**, *105*, 1–10. [[CrossRef](#)]
43. Xu, J.Q.; Wang, J.; Xiong, N.N.; Chen, Y.H.; Sun, L.; Wang, Y.T.; An, L.K. Analysis of Ecological Blockage Pattern in Beijing Important Ecological Function Area, China. *Remote. Sens.* **2022**, *14*, 1151. [[CrossRef](#)]
44. Zhang, X.C.; Ma, C.; Zhan, S.F.; Chen, W.P. Evaluation and simulation for ecological risk based on emergy analysis and Pressure-State-Response Model in a coastal city, China. *Procedia Environ. Sci.* **2012**, *13*, 221–231. [[CrossRef](#)]
45. Peng, Y.J.; Meng, M.H.; Huang, Z.H.; Wang, R.F.; Cui, G.F. Landscape Connectivity Analysis and Optimization of Qianjiangyuan National Park, Zhejiang Province, China. *Sustainability* **2021**, *13*, 5944. [[CrossRef](#)]
46. Tian, J.Y.; Gang, G.S. Research on Regional Ecological Security Assessment. *Energy Procedia* **2012**, *16*, 1180–1186. [[CrossRef](#)]
47. Yu, K. Security patterns and surface model in landscape ecological planning. *Landsc. Urban. Plan.* **1996**, *36*, 1–17. [[CrossRef](#)]
48. Dong, J.Q.; Peng, J.; Xu, Z.H.; Liu, Y.X.; Wang, X.Y.; Li, B. Integrating regional and interregional approaches to identify ecological security patterns. *Landsc. Ecol.* **2021**, *36*, 2151–2164. [[CrossRef](#)]
49. Zhang, J.X.; Cao, Y.M.; Ding, F.S.; Wu, J.; Chang, I.S. Regional Ecological Security Pattern Construction Based on Ecological Barriers: A Case Study of the Bohai Bay Terrestrial Ecosystem. *Sustainability* **2022**, *14*, 5384. [[CrossRef](#)]
50. Adriaensen, F.; Chardon, J.P.; De Blust, G.; Swinnen, E.; Villalba, S.; Gulinck, H.; Matthysen, E. The application of ‘least-cost’ modelling as a functional landscape model. *Landsc. Urban. Plan.* **2003**, *64*, 233–247. [[CrossRef](#)]
51. Ma, L.B.; Bo, J.; Li, X.Y.; Fang, F.; Cheng, W.J. Identifying key landscape pattern indices influencing the ecological security of inland river basin: The middle and lower reaches of Shule River Basin as an example. *Sci. Total. Environ.* **2019**, *674*, 424–438. [[CrossRef](#)] [[PubMed](#)]
52. Xia, M.; Wang, L.Y.; Wen, B.; Zou, W.; Ou, W.X.; Qu, Z.Q. Land Consolidation Zoning in Coastal Tidal Areas Based on Landscape Security Pattern: A Case Study of Dafeng District, Yancheng, Jiangsu Province, China. *Land* **2021**, *10*, 145. [[CrossRef](#)]
53. Li, Y.H.; Xiang, B.; Hu, Y. Establishment of Ecological Security Pattern for Suzhou National New & Hi-tech Industrial Development Zone. In *Applied Materials and Technologies for Modern Manufacturing*; Trans Tech Publications Ltd.: Stafa-Zurich, Switzerland, 2013; pp. 1371–1376.
54. Dai, Y. Identifying the ecological security patterns of the Three Gorges Reservoir Region, China. *Environ. Sci. Pollut. Res. Int.* **2022**, *29*, 45837–45847. [[CrossRef](#)] [[PubMed](#)]
55. Chen, L.; Li, Y.; Hu, Y.; Xiong, Z.; Wu, W.; Li, Y.; Wen, Q. Habitat selection by roe deer (*Capreolus pygargus*) over winter in the Tieli Forestry Bureau of the Lesser Xing’an Mountains. *Biodivers. Sci.* **2017**, *25*, 401–408.
56. Wu, J.S.; Zhang, S.Y.; Luo, Y.H.; Wang, H.L.; Zhao, Y.H. Assessment of risks to habitat connectivity through the stepping-stone theory: A case study from Shenzhen, China. *Urban. For. Urban. Green.* **2022**, *71*, 127532. [[CrossRef](#)]
57. Zhuang, Q.; Wang, L.; Zheng, G. An Evaluation of National Park System Pilot Area Using the AHP-Delphi Approach: A Case Study of the Qianjiangyuan National Park System Pilot Area, China. *Forests* **2022**, *13*, 1162. [[CrossRef](#)]
58. Du, A.; Xu, W.H.; Xiao, Y.; Cui, T.; Song, T.Y.; Ouyang, Z.Y. Evaluation of Prioritized Natural Landscape Conservation Areas for National Park Planning in China. *Sustainability* **2020**, *12*, 1840. [[CrossRef](#)]
59. Shu, H.; Xiao, C.W.; Ma, T.; Sang, W.G. Ecological Health Assessment of Chinese National Parks Based on Landscape Pattern: A Case Study in Shennongjia National Park. *Int. J. Environ. Res. Public Health* **2021**, *18*, 11487. [[CrossRef](#)]

60. Yang, D.C.; Gao, C.; Li, L.Y.; Van Eetvelde, V. Multi-scaled identification of landscape character types and areas in Lushan National Park and its fringes, China. *Landsc. Urban. Plan.* **2020**, *201*, 103844. [[CrossRef](#)]
61. Zhang, X.Y.; Ning, X.G.; Wang, H.; Zhang, X.Y.; Liu, Y.F.; Zhang, W.W. Quantitative assessment of the risk of human activities on landscape fragmentation: A case study of Northeast China Tiger and Leopard National Park. *Sci. Total. Environ.* **2022**, *85*, 158413. [[CrossRef](#)]
62. Ai, J.W.; Yu, K.Y.; Zeng, Z.; Yang, L.Q.; Liu, Y.F.; Liu, J. Assessing the dynamic landscape ecological risk and its driving forces in an island city based on optimal spatial scales: Haitan Island, China. *Ecol. Indic.* **2022**, *137*, 108771. [[CrossRef](#)]
63. Garcia-Llamas, P.; Calvo, L.; De la Cruz, M.; Suarez-Seoane, S. Landscape heterogeneity as a surrogate of biodiversity in mountain systems: What is the most appropriate spatial analytical unit? *Ecol. Indic.* **2018**, *85*, 285–294. [[CrossRef](#)]
64. Jin, Y.; Li, A.N.; Bian, J.H.; Nan, X.; Lei, G.B.; Muhammad, K. Spatiotemporal analysis of ecological vulnerability along Bangladesh-China-India-Myanmar economic corridor through a grid level prototype model. *Ecol. Indic.* **2021**, *120*, 106933. [[CrossRef](#)]
65. Zhang, Y.; Liu, X.N.; Yang, Q.; Liu, Z.L.; Li, Y. Extracting Frequent Sequential Patterns of Forest Landscape Dynamics in Fenhe River Basin, Northern China, from Landsat Time Series to Evaluate Landscape Stability. *Remote Sens.* **2021**, *13*, 3963. [[CrossRef](#)]
66. Kim, M.; Song, K.; Chon, J. Key coastal landscape patterns for reducing flood vulnerability. *Sci. Total. Environ.* **2021**, *759*, 143454. [[CrossRef](#)]
67. Bródka, S.; Kubacka, M.; Macias, A. Landscape Diversity and the Directions of Its Protection in Poland Illustrated with an Example of Wielkopolskie Voivodeship. *Sustainability* **2021**, *13*, 13812. [[CrossRef](#)]
68. Wei, S.; Pan, J.; Liu, X. Landscape ecological safety assessment and landscape pattern optimization in arid inland river basin: Take Ganzhou District as an example. *Hum. Ecol. Risk Assess. Int. J.* **2018**, *26*, 782–806. [[CrossRef](#)]
69. Duan, H.; Yu, X. Linking landscape characteristics to shorebird habitat quality changes in a key stopover site along the East Asian–Australasian Flyway migratory route. *Ecol. Indic.* **2022**, *144*, 109490. [[CrossRef](#)]
70. Rakoto, P.Y.; Deilami, K.; Hurley, J.; Amati, M.; Sun, Q. Revisiting the cooling effects of urban greening: Planning implications of vegetation types and spatial configuration. *Urban. For. Urban. Green.* **2021**, *64*, 127266. [[CrossRef](#)]
71. Han, R.-C.; Xiao, J.-X. Deciding Weighing by Entropy Value Method Is an Error. In Proceedings of the 2009 Second International Conference on Information and Computing Science, Manchester, UK, 21–22 May 2009; p. 255.
72. Lei, X.; Ouyang, H.; Xu, L. Image segmentation based on equivalent three-dimensional entropy method and artificial fish swarm optimization algorithm. *Opt. Eng.* **2018**, *57*, 103106. [[CrossRef](#)]
73. Abe, S.; Thurner, S. Robustness of the second law of thermodynamics under generalizations of the maximum entropy method. *Europhys. Lett.* **2008**, *81*, 10004. [[CrossRef](#)]
74. Wang, R.; Li, M.; Han, J.; Wang, C. Fitness relativity and path-dependent selection. *Biodivers. Sci.* **2022**, *30*, 21323. [[CrossRef](#)]
75. Dieni, J.S.; Jones, S.L. Grassland songbird nest site selection patterns in northcentral Montana. *Wilson Bull.* **2003**, *115*, 388–396. [[CrossRef](#)] [[PubMed](#)]
76. Stuber, E.F.; Fontaine, J.J. How characteristic is the species characteristic selection scale? *Glob. Ecol. Biogeogr.* **2019**, *28*, 1839–1854. [[CrossRef](#)]
77. Stuber, E.F.; Gruber, L.F.; Fontaine, J.J. Predicting species-habitat relationships: Does body size matter? *Landsc. Ecol.* **2018**, *33*, 1049–1060. [[CrossRef](#)]
78. Farina, A.; Pieretti, N.; Morganti, N. Acoustic patterns of an invasive species: The Red-billed Leiothrix (*Leiothrix lutea* Scopoli 1786) in a Mediterranean shrubland. *Bioacoustics* **2013**, *22*, 175–194. [[CrossRef](#)]
79. Pagani-Nunez, E.; Renom, M.; Furquet, C.; Rodriguez, J.; Llimona, F.; Senar, J.C. Isotopic niche overlap between the invasive leiothrix and potential native competitors. *Anim. Biodivers. Conserv.* **2018**, *41*, 427–434. [[CrossRef](#)]
80. Park, J.G.; Park, C.U.; Jin, K.S.; Kim, Y.M.; Kim, H.Y.; Jeong, S.Y.; Nam, D.H. Moulting and plumage patterns of the critically endangered Yellow-breasted Bunting (*Yellow-breasted bunting*) at a stopover site in Korea. *J. Ornithol.* **2019**, *161*, 257–266. [[CrossRef](#)]
81. Richard, K.; Ramellini, S.; Maziarz, M.; Pereira, P.F. The Red-billed Leiothrix (*Leiothrix lutea*): A new invasive species for Britain? *Ibis* **2022**, *164*, 1285–1294.
82. Bao, W.S.; Kathait, A.; Li, X.; Ozaki, K.; Hanada, Y.; Thomas, A.; Carey, G.J.; Gou, J.; Davaasuren, B.; Hasebe, M.; et al. Subspecies Taxonomy and Inter-Population Divergences of the Critically Endangered Yellow-breasted Bunting: Evidence from Song Variations. *Animals* **2022**, *12*, 2292. [[CrossRef](#)]
83. Li, Y.Y.; Zhang, Y.Z.; Jiang, Z.Y.; Guo, C.X.; Zhao, M.Y.; Yang, Z.G.; Guo, M.Y.; Wu, B.Y.; Chen, Q. Integrating morphological spatial pattern analysis and the minimal cumulative resistance model to optimize urban ecological networks: A case study in Shenzhen City, China. *Ecol. Process.* **2021**, *10*, 63. [[CrossRef](#)]
84. Wang, C.; Yang, Q.; Wu, S. Coordinated Development Relationship between Port Cluster and Its Hinterland Economic System Based on Improved Coupling Coordination Degree Model: Empirical Study from China’s Port Integration. *Sustainability* **2022**, *14*, 4963. [[CrossRef](#)]
85. Cheng, X.; Long, R.Y.; Chen, H.; Li, Q.W. Coupling coordination degree and spatial dynamic evolution of a regional green competitiveness system—A case study from China. *Ecol. Indic.* **2019**, *104*, 489–500. [[CrossRef](#)]
86. Li, Y.; Zhang, X.; Gao, X. An Evaluation of the Coupling Coordination Degree of an Urban Economy–Society–Environment System Based on a Multi-Scenario Analysis: The Case of Chengde City in China. *Sustainability* **2022**, *14*, 6790. [[CrossRef](#)]

87. Chen, P.; Shi, X. Dynamic evaluation of China's ecological civilization construction based on target correlation degree and coupling coordination degree. *Environ. Impact Assess. Rev.* **2022**, *93*, 106734. [[CrossRef](#)]
88. Jiang, L.L.; Wu, Y.X.; He, X.L.; Fu, Q.; Wang, Z.L.; Jiang, Q.X. Dynamic simulation and coupling coordination evaluation of water footprint sustainability system in Heilongjiang province, China: A combined system dynamics and coupled coordination degree model. *J. Clean. Prod.* **2022**, *380*, 135044. [[CrossRef](#)]
89. Liu, W.; Wang, J. Evaluation of coupling coordination degree between urban rail transit and land use. *Int. J. Commun. Syst.* **2021**, *34*, e4015. [[CrossRef](#)]
90. Zhou, J.L.; Fan, X.B.; Li, C.G.; Shang, G.F. Factors Influencing the Coupling of the Development of Rural Urbanization and Rural Finance: Evidence from Rural China. *Land* **2022**, *11*, 853. [[CrossRef](#)]
91. Kong, Q.S.; Kong, H.Y.; Miao, S.L.; Zhang, Q.; Shi, J.G. Spatial Coupling Coordination Evaluation between Population Growth, Land Use and Housing Supply of Urban Agglomeration in China. *Land* **2022**, *11*, 1396. [[CrossRef](#)]
92. Zhu, Y.; Wang, C.; Sakai, T. Remote Sensing-Based Analysis of Landscape Pattern Evolution in Industrial Rural Areas: A Case of Southern Jiangsu, China. *Sustainability* **2019**, *11*, 4994. [[CrossRef](#)]
93. Xu, L.T.; Chen, S.S.; Xu, Y.; Li, G.Y.; Su, W.Z. Impacts of Land-Use Change on Habitat Quality during 1985–2015 in the Taihu Lake Basin. *Sustainability* **2019**, *11*, 3513. [[CrossRef](#)]
94. Yeager, L.A.; Keller, D.A.; Burns, T.R.; Pool, A.S.; Fodrie, F.J. Threshold effects of habitat fragmentation on fish diversity at landscapes scales. *Ecology* **2016**, *97*, 2157–2166. [[CrossRef](#)] [[PubMed](#)]
95. Martinson, H.M.; Fagan, W.F. Trophic disruption: A meta-analysis of how habitat fragmentation affects resource consumption in terrestrial arthropod systems. *Ecol. Lett.* **2014**, *17*, 1178–1189. [[CrossRef](#)] [[PubMed](#)]
96. Fahrig, L. Effects of habitat fragmentation on biodiversity. *Annu. Rev. Ecol. Evol. Syst.* **2003**, *34*, 487–515. [[CrossRef](#)]
97. Yarnall, A.H.; Byers, J.E.; Yeager, L.A.; Fodrie, F.J. Comparing edge and fragmentation effects within seagrass communities: A meta-analysis. *Ecology* **2022**, *103*, e3603. [[CrossRef](#)] [[PubMed](#)]
98. Zhang, D.K.; Wang, J.P.; Wang, Y.; Xu, L.; Zheng, L.; Zhang, B.W.; Bi, Y.Z.; Yang, H. Is There a Spatial Relationship between Urban Landscape Pattern and Habitat Quality? Implication for Landscape Planning of the Yellow River Basin. *Int. J. Environ. Res. Public Health* **2022**, *19*, 11974. [[CrossRef](#)]
99. Benitez-Lopez, A.; Alkemade, R.; Verweij, P.A. The impacts of roads and other infrastructure on mammal and bird populations: A meta-analysis. *Biol. Conserv.* **2010**, *143*, 1307–1316. [[CrossRef](#)]
100. Lockhart, J.; Koper, N. Northern prairie songbirds are more strongly influenced by grassland configuration than grassland amount. *Landscape Ecol.* **2018**, *33*, 1543–1558. [[CrossRef](#)]
101. Copete, J.L. European breeding bird atlas 2. Distribution, abundance and change. *Ardeola-Int. J. Ornithol.* **2022**, *69*, 149–150.
102. Ramellini, S.; Simoncini, A.; Ficetola, G.F.; Falaschi, M. Modelling the potential spread of the Red-billed Leiothrix *Leiothrix lutea* in Italy. *Bird Study* **2019**, *66*, 550–560. [[CrossRef](#)]
103. Flyvbjerg, B.; Holm, M.K.S.; Buhl, S.L. Incorporating ecology into land use planning—The songbirds' case for clustered development—Response. *J. Am. Plan. Assoc.* **2003**, *69*, 83. [[CrossRef](#)]
104. Theobald, D.M.; Miller, J.R.; Hobbs, N.T. Estimating the cumulative effects of development on wildlife habitat. *Landscape Urban. Plan.* **1997**, *39*, 25–36. [[CrossRef](#)]
105. Herrando, S.; Vorisek, P.; Paquet, J.-Y.; Kupka, M.; Keller, V. The European Breeding Bird Atlas 2: From Wallonia and Brussels to Europe. *Aves* **2015**, *52*, 20–28.
106. Newton, I. Migration within the annual cycle: Species, sex and age differences. *J. Ornithol.* **2011**, *152*, 169–185. [[CrossRef](#)]
107. de la Hera, I.; Perez-Tris, J.; Telleria, J.L. Relationships among timing of moult, moult duration and feather mass in long-distance migratory passerines. *J. Avian. Biol.* **2010**, *41*, 609–614. [[CrossRef](#)]
108. Mlikovsky, J.; Styblo, P. Biometry, ecology and population status of the Endangered Yellow-breasted Bunting Yellow-breasted bunting in the Svyatoy Nos wetlands, Lake Baikal, eastern Siberia, Russia. *Forktail* **2016**, *32*, 1–4.
109. Kamp, J.; Opper, S.; Ananin, A.A.; Durnev, Y.A.; Gashev, S.N.; Holzel, N.; Mishchenko, A.L.; Pessa, J.; Smirenski, S.M.; Strelnikov, E.G.; et al. Global population collapse in a superabundant migratory bird and illegal trapping in China. *Conserv. Biol.* **2015**, *29*, 1684–1694. [[CrossRef](#)] [[PubMed](#)]

**Disclaimer/Publisher's Note:** The statements, opinions and data contained in all publications are solely those of the individual author(s) and contributor(s) and not of MDPI and/or the editor(s). MDPI and/or the editor(s) disclaim responsibility for any injury to people or property resulting from any ideas, methods, instructions or products referred to in the content.